Iron Carbide or Iron Carbide / Cobalt Nanoparticles for Magnetically-Induced CO 2 Hydrogenation over Ni/SiRAlOx Catalysts

Sumeet S Kale, Juan Manuel Asensio, Marta Estrader, Mayke Werner, Alexis Bordet, Deliang Yi, Julien Marbaix, Pier-Francesco Fazzini, Aikaterini Soulantika, Bruno Chaudret

Iron Carbide or Iron Carbide / Cobalt Nanoparticles for Magnetically-Induced CO_2 Hydrogenation over Ni/SiRAlOx Catalysts

Sumeet S. Kale, Juan M. Asensio, Marta Estrader,* Mayke Werner, Alexis Bordet, Deliang Yi, Julien Marbaix, Pier-Francesco Fazzini, Katerina Soulantica* and Bruno Chaudret.**

LPCNO, Université de Toulouse, CNRS, INSA, UPS, 135 avenue de Rangueil, 31077 Toulouse, France.

*Dr Juan M. Asensio: asensior@ insa-toulouse.fr

*Dr. Bruno Chaudret: chaudret@insa-toulouse.fr

*Dr. Katerina Soulantica: ksoulant@insa-toulouse.fr

*Dr. Marta Estrader: martaestrader@gmail.com

ABSTRACT. Magnetic nanoparticles heve recently been used as heating agents in heterogeneously catalyzed reactions such as CO_2 hydrogenation into methane. In the present work, we explore the potential of heating agents presenting different heating properties in the activation of a supported catalyst based on nickel nanoparticles (NPs) (Ni/SiRAlOx) for the CO_2 methanation under continuous flow. Two types of $Fe_{2.2}C$ NPs presenting distinct heating properties have been tested. For $Fe_{2.2}C$ NPs displaying lower heating powers of ca. 1 $kW \cdot g^{-1}$, an activation of the catalyst at a magnetic field amplitude of 80 mT is necessary to achieve high conversion and selectivity, this activation step being attributed to a partial sintering of the Ni NPs. When using $Fe_{2.2}C$ NPs displaying much higher heating powers of 2 $kW \cdot g^{-1}$ as heating agents, the magnetic field amplitude required to activate the catalyst can be reduced to 48 mT. Finally, we demonstrate that *hard* magnetic materials displaying very low heating power but high Curie temperatures, such as Co nanorods (NRs), can be used as relay heating agents when mixed with small amounts of *softer* materials with high heating power. Thus, by mixing Co NRs with $Fe_{2.2}C$ NPs, excellent catalytic performances (90 % of CO_2 and 100%

CH_4 selectivity) have been obtained after applying only 32 mT to trigger the reaction. Once the reaction initiated, these performancesare maintained even after lowering the magnetic field to 16 mT, which is advantageous in terms of energy consumption.

INTRODUCTION

As a consequence of the fast development of global energy consumption, CO_2 emissions are continuously increasing, hence enhancing the greenhouse effect.[1, 2] Thus, research efforts have as an objective the use of CO_2 as a chemical feedstock to produce platform molecules or fuels.[3-6] A possible way to use CO_2 is the catalytic hydrogenation (Sabatier process[7, 8]) for methane production, the so-called synthesis of natural gas (SNG). The process is industrially applicable, and favorable in terms of carbon balance, provided that the hydrogen is obtained from renewable and sustainable sources (e.g. photocatalysis or electrocatalytisis of water powered by wind/solar energy, biomass, etc.).[9, 10] CO_2 methanation is a reversible and strongly exothermic reaction.[11] Although it is thermodynamically favorable, the high kinetic barrier for the activation of CO_2 is the main challenge to achieve high CH_4 yields at low temperatures.[12-14] Hence, selecting the appropriate catalyst is the key step to overcome the kinetic limitation. During the past years, several supported metal-based catalysts have been investigated, in particular, transition metals such as Ni, Fe, Co, Ru, Rh, etc. dispersed on various supports like Al_2O_3, SiO_2, TiO_2, ZrO_2, CeO_2, etc.[11, 15] Among them, Ni based catalysts are the most widely studied due to the best trade-off between activity and cost.[16] Traditionally, CO_2 methanation is performed in a continuous flow reactor using conventional heating.

Magnetic hyperthermia has been applied in the field of cancer therapy,[17-20] but it has been shown recently that the same principle can also be advantageously applied in heterogeneous catalysis.[21-29] The concept is based on the fact that ferromagnetic materials placed in a high-frequency alternating magnetic field release heat through hysteresis losses. Hence, by using

magnetic nanoparticles (NPs) the heat is directly and homogeneously distributed within the catalyst without the need for heating the whole reactor system. In addition, magnetic induction heating allows reaching the target temperature in a few seconds, which makes the system well-adapted to intermittent energies. Magnetically induced catalysis requires the design of catalytic systems combining good heating capacity with high catalytic activity. The heating efficiency of metallic NPs is quantified by the specific absorption rate (SAR), which represents the amount of energy absorbed per unit of mass in the presence of an alternating magnetic field and can be measured in units of watts per gram of metal ($W \cdot g^{-1}$). Recently, we have reported the synthesis of FeCx NPs with ca. 15 nm mean size displaying much higher heating properties than any previously described material. The NPs were synthesized by the carbidization of pre-formed monodisperse Fe(0) NPs by a mixture of *syngas* (CO/H_2). The very high SAR values were ascribed to the presence of crystalline $Fe_{2.2}C$. [26, 30]

However, the heating power of magnetic materials is reduced with increasing temperature as a result of the reduction of the area of the hysteresis loop and becomes zero at the Curie Temperature. For FeCx, the Curie temperature (T_C) is close to 450 ºC[31, 32], depending on the exact stoichiometry of the carbide and therefore, the heating power will start to decrease at high temperatures. Thus, ferromagnetic materials with higher *T*c values may retain a large enough coercive field to allow efficient heating at lower magnetic field amplitudes even at high temperature. For example, Co is a *hard* magnetic material with a high magnetocrystalline anisotropy and a high Curie Temperature (T_C > 1000 °C[33]), which would require at room temperature very high field amplitudes to release heat and, therefore, which cannot be used for heat production. However, by combining *hard* and *soft* magnetic materials in a single hybrid object,[34] the anisotropy of the whole system may be reduced, leading to a material that would be activated at lower magnetic field amplitudes.[35, 36] A different configuration would be a simple mixing of *hard* and *soft* nanomaterials that do not interact directly and which

could allow upon magnetic excitation a pre-heating of the *hard* material through the heat released by the soft material. This would in turn decrease the coercivity of the *hard* material and render magnetic heating by the *hard* heating agent possible. In this respect, *hcp*-Co nanorods (Co NRs) previously prepared in our laboratory are good candidates to act as a *hard* ferromagnetic material, as they possess high magnetocrystalline and shape anisotropies, and hence high values of coercive fields (Hc).[37, 38] $Fe_{2.2}C$ NPs could then function as "starters" for reaching the temperature above which Co NRs can be easily activated by lower magnetic fields.

In a previous report from our group, we have demonstrated the possibility to magnetically induce CO_2 methanation in a continuous-flow reactor.[26] In that work, core@shell $Fe_{2.2}C$@Ni NPs/SiRAlOx led to solely 50% of CO_2 conversion with a CH_4 yield of 15% when applying 40 mT. However, a catalyst composed of Ru NPs supported on SiRAlOx on which $Fe_{2.2}C$ NPs were present but without being directly associated to Ru, presented 93% of CO_2 conversion with a 100% selectivity to CH_4, when activated by an external magnetic field of only 28 mT. Therefore, a direct contact between the heating agent ($Fe_{2.2}C$ NPs) and the catalyst Ru NPs is not indispensable for obtaining good catalytic performances.

Considering that Ni is a good catalyst for the Sabatier reaction, and that a mixture of $Fe_{2.2}C$ NPs and Ni NPs immobilized on SiRAlOx ($Fe_{2.2}C$/Ni/SiRAlOx) is a simpler system than the one based on $Fe_{2.2}C$@Ni NPs immobilized on SiRAlOx, in the present study and in search for an optimized system, we have designed a new catalytic system consisting of Ni NPs supported on SiRAlOx (**Ni/SiRAlOx**) which was associated to $Fe_{2.2}C$ NPs as a heating agent. The catalytic activity has been assessed as a function of the SAR values of $Fe_{2.2}C$ NPs and the presence or not of a pre-activation step for **Ni/SiRAlOx**. Furthermore, we explore here the concept of implementing *hard* magnetic *hcp*-Co NRs as a stable heating source by using small amounts of a *soft* magnetic material ($Fe_{2.2}C$ NPs) as initiators.

.

RESULTS AND DISCUSSION

Catalytic activity of Ni/SiRAlOx in CO_2 hydrogenation through conventional heating.

Ni/SiRAlOx was prepared simply by heating a mesitylene solution of $Ni(COD)_2$ at 150°C (see Experimental Section and Fig. S1 ESI†) in the presence of the support. The Scanning Transmission Electron Microscopy (STEM) images of **Ni/SiRAlOx** (Fig. S2) show the presence of crystalline Ni NPs on SiRAlOx. To confirm the metal composition and distribution of this phase along the SiRAlOx support, TEM and STEM-HAADF (High Angle Annular Dark Field) images combined with Energy-Dispersive X-Ray Spectroscopy (EDX) were recorded (Fig. S3), revealing the presence of Ni NPs with a mean size of 2-3 nm over the whole support.

The **Ni/SiRAlOx** catalyst (400 mg) was first tested in a conventional heating set-up. The catalytic activity was evaluated at ambient pressure in the temperature range of 300 °C to 450 °C (Fig. 1). A H_2:CO_2 molar ratio of 4:1 in a continuous flow set-up, with a total flow rate of 25 $mL \cdot min^{-1}$, was used throughout the experiment.

The results show that **Ni/SiRAlOx** is an active catalyst for CO_2 hydrogenation, the optimal global temperature of the catalyst (for conversions higher than 80%) being above 300 ºC. Increasing the temperature from 300 °C to 400 °C leads to an increase in CO_2 conversion with the simultaneous enhancement in CH_4 yield. A very high CO_2 conversion (> 95%) was observed at a set up temperature of 400 °C (376 °C measured by a thermocouple inside the reactor), with almost 99% selectivity to CH_4 formation. Further increase in temperature to 450 °C had no important influence on the reaction. Thanks to the presence of a water trap in the reactor, water removal shifts the equilibrium toward the formation of CH_4, thus, conversion

values are better than the anticipated ones based on the thermodynamic equilibrium values (description of the reactor is given in ESI-14).

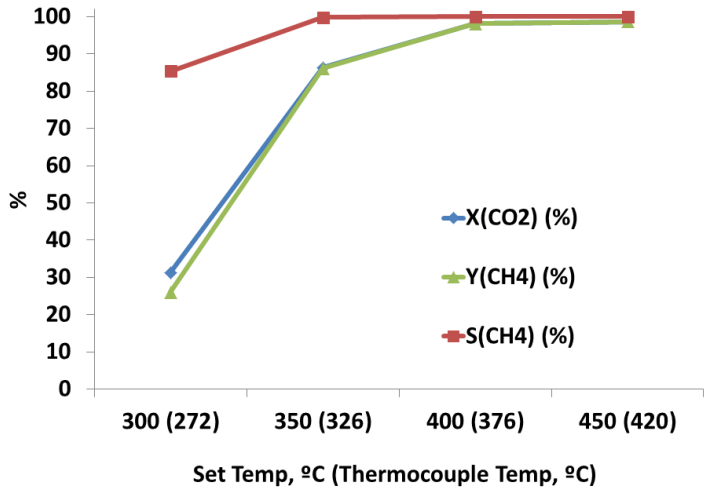

Figure 1. Catalytic results with **Ni/SiRAlOx** as a function of temperature in conventional heating.

Catalytic activity of Ni/SiRAlOx in CO_2 hydrogenation by magnetic heat induction

Three different magnetic heating agents were used in the following catalytic experiments, two types of $Fe_{2.2}C$ NPs and *hcp*-Co NRs. $Fe_{2.2}C$ NPs with a mean size of ca. 14-15 nm were synthesized through carbidization of pre-formed Fe(0) NPs of ca. 12.5 nm (see Fig. S4-6) under *syngas* ($CO:H_2$) following a recently described procedure (see Experimental Section). In our previous work, we have observed that dipolar couplings strongly affect the heating power displayed by $Fe_{2.2}C$ NPs. Thus, the SAR of the $Fe_{2.2}C$ NPs can be modulated by adjusting the amount of ligands at the beginning of the carbidization which permits preparing NPs with controllable heating powers.[39] In this respect $Fe_{2.2}C$ NPs displaying SAR values of ca. 1100 $W \cdot g^{-1}$ (**FeC-1)** and ca. 2100 $W \cdot g^{-1}$ (**FeC-2**) were synthesized, both measured at 47 mT with a frequency of 93 kHz (see Fig. S7-14). *hcp*-Co NRs were prepared following a previously reported method [40] (see Experimental Section and Fig. S15-16). Three catalytic

mixtures were tested. They were composed of the above-mentioned **Ni/SiRAlOx** catalyst which was then mixed (i) with $Fe_{2.2}C$ NPs, (ii) with *hcp*-Co NRs and (iii) with both $Fe_{2.2}C$ NPs and *hcp*-Co NRs (see Experimental section for details). The list of these catalysts and their abbreviations along with the corresponding ICP analyses are given in Table 1.

The CO_2 hydrogenation activity of the prepared samples was evaluated in a glass reactor (Internal Diameter of 1 cm) with a H_2:CO_2 molar ratio of 4:1 in a continuous flow under ambient pressure using an alternating magnetic field oscillating at a frequency (*f*) of 300 kHz. The total flow rate was set to 25 $mL \cdot min^{-1}$ throughout the experiments. The magnetic field was varied between 0 and 80 mT, and for each amplitude value it was maintained constant for one hour during which 3 injections into the Gas Chromatograph (GC) were performed.

Table 1. List of catalysts and their abbreviations used in the CO_2 methanation and ICP analyses.

No	Catalysts	Name	wt% Fe	wt% Ni	wt% Co
1	Ni/SiRAlOx	**Ni/SiRAlOx**	-	9.86	-
2	Ni/SiRAlOxpre-activated [a]	**Ni-pre**	-	n. a.	
3	**FeC-1** (SAR~1100 $W \cdot g^{-1}$)[b] on Ni/SiRAlOx	**FeC-1/Ni**	9.57	7.31	-
4	**FeC-2** (SAR~2100 $W \cdot g^{-1}$)[b] on Ni/SiRAlOx	**FeC-2/Ni**	8.92	7.01	-
5	**FeC-1** (SAR~1100 $W \cdot g^{-1}$) on **Ni-pre**	**FeC-1/Ni-pre**	6.83	6.37	-
6	**Co-NRs** on Ni/SiRAlOx	**Co/Ni**	-	-	9[c]
7	**Co-NRs** on Ni/SiRAlOx + **FeC-1** (SAR~1100 $W \cdot g^{-1}$) on SiRAlOx	**Co-FeC-1/Ni**	1.45	5.86	6.60

a) Pre-activated in the oven at 400 ºC. b) SAR measured in mesitylene solution at a $\mu_0 H_{rms}$ of 47 mT and a *f* of 93 kHz. c) Estimated from Thermogravimetric Analysis

$Fe_{2.2}C$ NPs as heating agent supported on Ni/SiRAlOx as catalyst (FeC/Ni) in magnetically induced CO_2 hydrogenation

The first configuration was explored with the two types of $Fe_{2.2}C$ NPs (**FeC-1** and **FeC-2**) described hereabove and differing by their heating capacities. The catalysts were elaborated by supporting $Fe_{2.2}C$ NPs on **Ni/SiRAlOx** hereafter called **FeC-1/Ni** and **FeC-2/Ni** (see Figures S17-18). First, we studied the CO_2 hydrogenation under continuous flow using 400 mg of **FeC-1/Ni** as catalyst. The $Fe_{2.2}C$ loadings were fixed to 10 wt%, as this concentration is close to the minimum required to activate the reaction.[26] Heating agent loadings of 5 wt% were not enough to reach the working temperatures (see below), whereas $Fe_{2.2}C$ loadings above 10 wt% did not have a significant influence on the CO_2 conversion. The temperature at the surface of the reactor was monitored using an infrared (IR) camera (see ESI-14). The magnetic field amplitude was set to 48 mT, a value at which the reactor temperature measured by the IR camera was found in the range of 240-260 °C. A rather low (35%) CO_2 conversion was obtained, although the catalyst was highly selective towards CH_4 formation. Subsequently, the magnetic field was set to 80 mT, where the catalyst showed a remarkable improvement in CO_2 conversion to 85% with a 99% selectivity to CH_4. At this point the temperature measured by thermal camera was 280 °C. It should be noted that the local temperature at the surface of the catalyst must be well-above that measured with the thermal camera. Thus, to obtain a similar conversion through conventional heating an oven temperature of 350 ºC should be set (see Fig 1). Interestingly, after this step, the reaction temperature, the CO_2 conversion and the selectivity for CH_4 remained stable even upon reducing the magnetic field down to 48 mT. As the global temperature of the reactor was comparable when applying a $\mu_0 H_{rms}$ of 48 or 80 mT, and the temperature necessary to activate CO_2 was reached at 48 mT before increasing the magnetic field up to 80 mT, the

improvement of the performance after activation of the catalyst is probably related to a change in the catalyst structure. This fact indicates that there is an induction step that corresponds to the activation of the catalyst. After catalyst activation, the catalytic activity was evaluated by varying the magnetic field from 16 mT to 80 mT, maintaining each value constant for at least 45 minutes (see Figure 2a). The CO_2 conversion was found to be above 70% in all the cases and a maximum value of 85% was obtained at 48 mT. The CH_4 selectivity was above 99% even at low magnetic field amplitudes. Finally, the stability of the catalyst **FeC-1/Ni** was evaluated by stopping the application of the magnetic field, stopping the CO_2 flow and cooling down to room temperature under inert atmosphere, and then restarting. The system maintained its catalytic activity exhibiting the same reaction profile as a function of the magnetic field but without the need for catalyst activation.

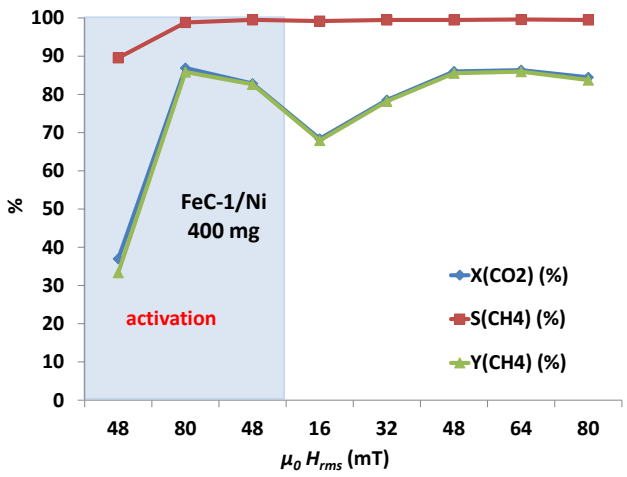

Figure 2. Magnetically induced hydrogenation of CO_2 using $Fe_{2.2}C$ NPs **FeC-1** as heating agents. CO_2 conversion, CH_4 yield and CH_4 selectivity as a function of magnetic field when using 400 mg of catalyst.

The residence time or weight hour space velocity (WHSV) of the gas flow was optimized for **FeC-1** (see Fig. S19). When using 300 mg of the **FeC-1/Ni** catalyst (ca. 1.2 cm of catalyst-bed

height), a significant decrease in CO_2 conversion (35%), CH_4 yield (30%) and CH_4 selectivity (70-80%) was observed both at 48 and 80 mT, producing CO as by-product. However, the temperature of the reactor was similar to that measured when employing 400 mg of catalyst, suggesting that the differences were more related to WHSV rather than to the temperature. In addition, the catalyst notably improved its performance after addition of 100 mg of the same batch of **FeC-1/Ni**. When performing the reaction using 600 mg of the catalyst **FeC-1/Ni** (ca. 2.3 cm of length), CO_2 conversion and CH_4 selectivity reached values of 88% and 99% respectively at 48 mT, without the need of any activation of the catalyst at 80 mT. Further variation on the magnetic field did not affect the performance of the catalyst.

TEM images of the spent catalysts (see Fig. S20-22) evidence changes in their morphology (see Fig. 3). STEM-BF, STEM-HAADF and EDX images show that Fe is present in large particles between 20 and 200 nm homogeneously distributed throughout the SiRAlOx support whereas Ni is mainly concentrated in big polydisperse aggregates of 5-100 nm (see Figure 3c and d) due to sintering of the Ni NPs at the high temperatures induced by the applied magnetic field.

Assuming that sintering of the NPs plays a role in the performance of the catalysts, **Ni/SiRAlOx** was thermally pre-treated in the presence of H_2 for 1 h at 400 °C, a temperature similar to the global temperature reached during the catalytic experiments, to give the sample **Ni-pre**. As can be observed by TEM and STEM-EDX mapping (see Fig. S23-25), a coalescence of the Ni NPs occurred to give big nano-objects in the range of 5-50 nm. **FeC-1** NPs were subsequently supported on **Ni-pre** and 400 mg of **FeC-1/Ni-pre** catalyst (see Fig. S26-28) were evaluated in CO_2 hydrogenation under the same conditions of flow and magnetic field previously described. Interestingly, CO_2 conversion was 73% with nearly 100% selectivity to CH_4 at 48 mT (see figure 4). The catalyst was then submitted to different magnetic fields (16 mT to 80 mT). A remarkable CO_2 conversion of 80% was obtained at 16

mT further supporting that the activation step needed for **the FeC-1/Ni** catalyst is linked to the sintering of Ni. This is in agreement with a recent report which showed that larger Ni NPs can afford better conversions in CO_2 methanation because CO adsorption, which is the rate-limiting step, is more efficient in that case.[41]

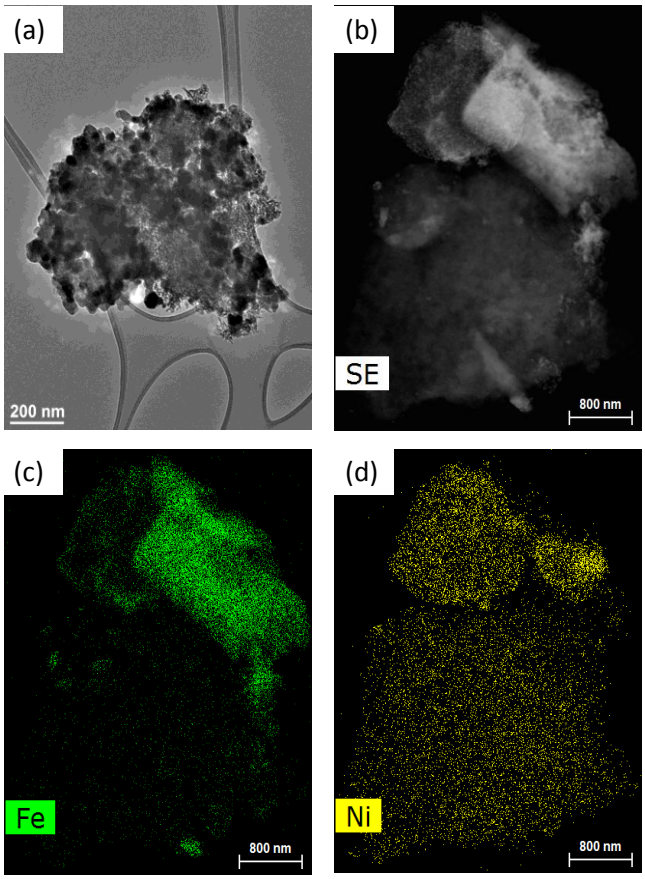

Figure 3. Characterization by HR-TEM of **FeC-1/Ni** after catalysis: (a) STEM-BF (Bright field) (b) STEM-HAADF (High angle annular dark field) and (c-d) EDX mapping showing the elements (c) Fe and (d) Ni.

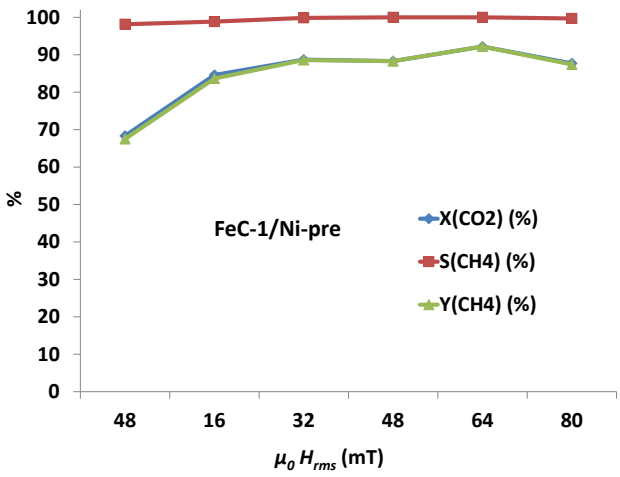

Figure 4. Magnetically induced hydrogenation of CO_2 using **FeC-1/Ni-pre** as catalyst.

Having optimized the catalytic procedure, we then evaluated the performance of the **FeC-2/Ni** catalyst in which the iron carbide NPs display a much better SAR value of ca. 2100 $W \cdot g^{-1}$. High CO_2 conversion (94%) and CH_4 selectivity (97%) were obtained, even when a magnetic field of 48 mT was directly applied without previous activation at 80mT. The reaction temperatures measured by thermal camera are in the same range (280-300 °C) as for **FeC-1/Ni** after the activation step. Increasing the magnetic field amplitude to 80 mT did not result in significant changes neither in the reaction temperature, nor in the CO_2 conversion and CH_4 selectivity, and these performances remained stable when decreasing the field back to 48 mT (Figure 5). These results indicate that, in contrast to **FeC-1/Ni**, the **FeC-2/Ni** sample reaches its maximum catalytic performance at lower magnetic field amplitudes (48mT) when using 400 mg of catalyst. As in the previous case, the catalytic activity was further investigated by gradually varying the magnetic field from 16 mT to 80 mT. The CH_4 selectivity reaches 100% above 32 mT with only a slight variation in CO_2 conversion, which was of more than 90% in all the cases. The catalyst was also found to be more active at 16 mT than **FeC-1/Ni**.

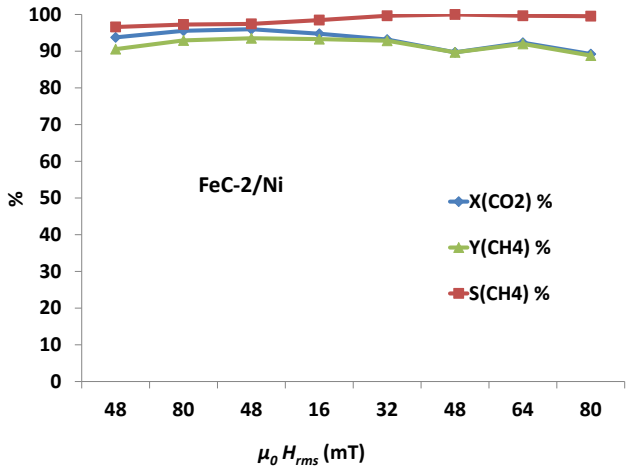

Figure 5. Magnetically induced hydrogenation of CO_2 using **FeC-2/Ni** as catalyst.

TEM micrographs evidenced that, similarly to **FeC-1/Ni**, **FeC-2/Ni** NPs were completely sintered after the catalytic reaction (see Fig S29). The rather small differences in the catalytic activity between **FeC-1/Ni-pre** and **FeC-2/Ni** in the long term (85% and 90% of CO_2 conversion at 16 mT for **FeC-1/Ni-pre** and **FeC-2/Ni**, respectively) suggest that the SAR of $Fe_{2.2}C$ NPs does not dramatically affect the performances of the catalyst once activated. However, the advantage of using $Fe_{2.2}C$ NPs with a higher SAR is the absence of activation step.

Co NRs supported on Ni/SiRAlOx as heating agent in magnetically induced CO_2 hydrogenation.

Aiming at exploring other nanomaterials as heating agents for magnetically induced catalysis, Co NRs were assessed as they possess a high T_C (> 1000 °C) in contrast to $Fe_{2.2}C$ NPs. Briefly, pre-synthesized Co NRs of ca. 80-90 nm length (see Experimental Section for synthesis details and SI for TEM and Vibrating Sample Magnetometry characterization, Fig. S15-16), were supported on **Ni/SiRAlOx** to afford the catalyst **Co/Ni** (Fig. S30). 300 mg of the latter were placed inside the glass reactor and 25 $mL \cdot min^{-1}$ of a 4:1 mixture of H_2:CO_2

were flowed through. Although the magnetic field was varied from 0 to the highest possible value, i.e. 80 mT, as expected, no variation of the temperature was observed during the experiment (see Fig. 6). Thus, owing to their high magnetocrystalline and shape anisotropies, Co NRs need much higher applied magnetic fields to start the rotation of the magnetic moment which is fixed along the easy magnetization axis (the long axis of the nanorod). Given that the magnetocrystalline anisotropy decreases with temperature, it is reasonable to anticipate that at higher temperature, the rotation of the magnetic moment of the NRs could be triggered, enabling the use of Co NRs as heating agents. For this to occur, a magnetically softer heating source, namely $Fe_{2.2}C$ NPs, should act as a preheating agent of the Co NRs. Hence, 300 mg of Co-NRs on **Ni/SiRAlOx (Co/Ni)** and 100 mg of **FeC-1/SiRAlOx** were mechanically mixed to give the catalyst **Co-FeC-1/Ni**. The latter was placed inside the reactor in the presence of a CO_2/H_2 flow and submitted to a magnetic field of 32 mT, which was the minimum field required to activate the system. Under these conditions, the measured temperature increased up to 280-300 ºC, leading to 88% of CO_2 conversion and 97% selectivity to CH_4 (see Fig 7). Importantly, by subsequently decreasing the magnetic field down to 16 mT, both CO_2 conversion (90%) and selectivity to CH_4 (100%) increased, even though the measured temperature slightly decreased (260 ºC). As T_c for Co is above the melting point of the glass and to avoid reactor melting, the field amplitude was not increased further. As a control experiment, the reaction was carried out under the same conditions after mixing 200 mg of **Ni/SiRAlOx** and 200 mg of **FeC-1/Ni** (approx. 5 wt% of Fe). In this case, the measured temperatures were always below 200 ºC and marginal CO_2 conversions were obtained (less than 5%). This experiment demonstrates that Co NRs are acting as relay heating agent for CO_2 hydrogenation. **Co-FeC-1/Ni** is envisaged as a good catalyst candidate for chemical reactions requiring high temperatures, such as methane dry reforming. The stability of **Co-FeC-1/Ni** catalyst over time was evaluated at 16 mT for 2 hours. A slight

decrease in CO_2 conversion, probably related to water accumulation in the reactor trap, was observed. After the catalysis, Co NRs and $Fe_{2.2}C$ NPs are no longer present, only big nano-objects being observed (Fig. S31).

Finally, 400 mg of the **Co-FeC-1/Ni** catalyst were evaluated in CO_2 hydrogenation through conventional heating under the same values of flow rate. The reaction profile as a function of temperature of **Co-FeC-1/Ni** was comparable to the one obtained with the **Ni/SiRAlOx** (see Fig S32), although the selectivity to CH_4 was slightly lower at high temperatures (ca. 95% at T=380 ºC). These results suggest that the presence of $Fe_{2.2}C$ NPs and Co NRs does not have a strong influence on the catalytic performance of **Ni/SiRAlOx.**

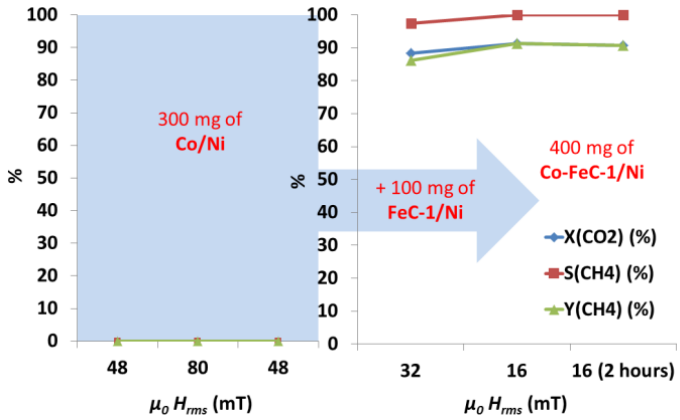

Figure 6. Magnetically induced hydrogenation of CO_2 using **Co/Ni** and **Co-FeC-1/Ni** as catalysts.

CONCLUSIONS

In this study, we show that magnetically induced heating can trigger CO_2 methanation catalyzed by supported Ni catalysts. Once the temperature needed for the reaction onset is reached, the energy is directly transferred to the catalyst, and the warming up of the reactor (20-30 seconds) is fast without the need to heat the reactor walls. The choice of the heating agent determines the magnetic field amplitude necessary for the catalyst to become

operational. As heating agents, we have used either *soft* magnetic $Fe_{2.2}C$ NPs or the combination of $Fe_{2.2}C$ NPs with the *hard* magnetic *hcp*-Co NRs (**Co-FeC-1/Ni**). In contrast to the $Fe_{2.2}C$@Ni NPs previously reported by our group, where both the catalytic and the heating agent were part of a single nano-object, in the current systems the two components are separated, which constitutes an advantage as this system is a simpler catalyst. Furthermore, combining a magnetically hard (Co NRs) and a magnetically soft material ($Fe_{2.2}C$ NPs) as heating agents permits exploiting the soft material to attain a temperature necessary for the hard material to start heating. Thus, for the combined **Co-FeC-1/Ni** system, excellent catalytic performances (90 % of CO_2 and 100% CH_4 selectivity) are achieved even at a very low field, namely 16 mT. This value allows a reduction of energy by a factor of 2. Optimization of the reaction conditions has allowed to improve the performance of the magnetically induced CO_2 methanation (low magnetic fields and small amounts of catalysts). Last but not least, as the T_c of Co overpasses 1000 °C, this combined material is a promising catalyst for chemical reactions requiring high temperatures such as methane reforming.

CONCFLICTS OF INTEREST

The authors declare no conflict of interest

AKNOWLEDGMENTS

The authors thank ERC Advanced Grant (MONACAT 2015-694159), Region Occitanie (HYDROMET) for financial support. M.E. thanks the European Union's Horizon 2020 research and innovation programme (Marie Skłodowska-Curie grant agreement No 704098). D. Yi thanks the ANR for financing the DENSAR project (ANR-14-CE07-0025-01). M. Werner thanks Toulouse Tech Transfer.

NOTES AND REFERENCES

1. M. Younas, L. Loong Kong, M. J. K. Bashir, H. Nadeem, A. Shehzad and S. Sethupathi, *Energy Fuels*, 2016, **30**, 8815-8831.
2. M. Younas, M. Sohail, L. K. Leong, M. J. K. Bashir and S. Sumathi, *Int. J. Environ. Sci. Technol.*, 2016, **13**, 1839-1860.
3. C. Ampelli, S. Perathoner and G. Centi, *Philos. Trans. R. Soc., A*, 2015, **373**, 1-35.
4. G. Centi, E. A. Quadrelli and S. Perathoner, *Energy Environ. Sci.*, 2013, **6**, 1711-1731.
5. E. V. Kondratenko, G. Mul, J. Baltrusaitis, G. O. Larrazabal and J. Perez-Ramirez, *Energy Environ. Sci.*, 2013, **6**, 3112-3135.
6. S. Saeidi, S. Najari, F. Fazlollahi, M. K. Nikoo, F. Sefidkon, J. J. Klemes and L. L. Baxter, *Renewable Sustainable Energy Rev.*, 2017, **80**, 1292-1311.
7. P. Sabatier and J. B. Senderens, *C. R. Hebd. Seances Acad. Sci.*, 1902, **134**, 689.
8. J. Kirchner, J. K. Anolleck, H. Loesch and S. Kureti, *Appl. Catal., B*, 2018, **223**, 47-59.
9. G. Gahleitner, *Int. J. Hydrogen Energy*, 2013, **38**, 2039-2061.
10. S. Schiebahn, T. Grube, M. Robinius, V. Tietze, B. Kumar and D. Stolten, *Int. J. Hydrogen Energy*, 2015, **40**, 4285-4294.
11. J. Gao, Q. Liu, F. Gu, B. Liu, Z. Zhong and F. Su, *RSC Adv.*, 2015, **5**, 22759-22776.
12. W. Wang and J. Gong, *Front. Chem. Sci. Eng.*, 2011, **5**, 2-10.
13. W. Wang, S. Wang, X. Ma and J. Gong, *Chem. Soc. Rev.*, 2011, **40**, 3703-3727.
14. J.-N. Park and E. W. McFarland, *J. Catal.*, 2009, **266**, 92-97.
15. M. A. A. Aziz, A. A. Jalil, S. Triwahyono and A. Ahmad, *Green Chem.*, 2015, **17**, 2647-2663.
16. L. Xu, F. Wang, M. Chen, J. Zhang, K. Yuan, L. Wang, K. Wu, G. Xu and W. Chen, *RSC Adv.*, 2016, **6**, 28489-28499.
17. D. H. Ortgies, F. J. Teran, U. Rocha, L. de la Cueva, G. Salas, D. Cabrera, A. S. Vanetsev, M. Rähn, V. Sammelselg, Y. V. Orlovskii and D. Jaque, *Advanced Functional Materials*, 1704434-n/a.
18. J. Yu, F. Chen, W. Gao, Y. Ju, X. Chu, S. Che, F. Sheng and Y. Hou, *Nanoscale Horiz.*, 2017, **2**, 81-88.
19. E. A. Perigo, G. Hemery, O. Sandre, D. Ortega, E. Garaio, F. Plazaola and F. J. Teran, *Appl. Phys. Rev.*, 2015, **2**, 041302/041301-041302/041335.
20. E. C. Abenojar, S. Wickramasinghe, J. Bas-Concepcion and A. C. S. Samia, *Prog. Nat. Sci.: Mater. Int.*, 2016, **26**, 440-448.
21. S. Ceylan, C. Friese, C. Lammel, K. Mazac and A. Kirschning, *Angew. Chem., Int. Ed.*, 2008, **47**, 8950-8953.
22. S. Ceylan, L. Coutable, J. Wegner and A. Kirschning, *Chem. - Eur. J.*, 2011, **17**, 1884-1893, S1884/1881-S1884/1818.
23. J. Hartwig, S. Ceylan, L. Kupracz, L. Coutable and A. Kirschning, *Angew. Chem., Int. Ed.*, 2013, **52**, 9813-9817.
24. WO2014162099A1, 2014.
25. A. Meffre, B. Mehdaoui, V. Connord, J. Carrey, P. F. Fazzini, S. Lachaize, M. Respaud and B. Chaudret, *Nano Lett.*, 2015, **15**, 3241-3248.
26. A. Bordet, L.-M. Lacroix, P.-F. Fazzini, J. Carrey, K. Soulantica and B. Chaudret, *Angew. Chem., Int. Ed.*, 2016, **55**, 15894-15898.
27. P. M. Mortensen, J. S. Engbaek, S. B. Vendelbo, M. F. Hansen and M. Oestberg, *Ind. Eng. Chem. Res.*, 2017, **56**, 14006-14013.
28. A. Bordet, J. M. Asensio, K. Soulantica and B. Chaudret, *ChemCatChem*, 2018, **10**, 4047-4051.

29. M. G. Vinum, M. R. Almind, J. S. Engbaek, S. B. Vendelbo, M. F. Hansen, C. Frandsen, J. Bendix and P. M. Mortensen, *Angew. Chem., Int. Ed.*, 2018, **57**, 10569-10573.
30. A. Bordet, L.-M. Lacroix, K. Soulantica and B. Chaudret, *ChemCatChem*, 2016, **8**, 1727-1731.
31. L. J. E. Hofer, E. M. Cohn and W. C. Peebles, *J. Am. Chem. Soc.*, 1949, **71**, 189-195.
32. G. Le Caer, J. M. Dubois, M. Pijolat, V. Perrichon and P. Bussiere, *J. Phys. Chem.*, 1982, **86**, 4799-4808.
33. H. P. R. Frederikse, in *CRC Handbook of Chemistry and Physics*, ed. D. R. Lide, CRC Press, Boca Raton, FL, 2009.
34. N. Liakakos, C. Gatel, T. Blon, T. Altantzis, S. Lentijo-Mozo, C. Garcia-Marcelot, L.-M. Lacroix, M. Respaud, S. Bals, G. Van Tendeloo and K. Soulantica, *Nano Lett.*, 2014, **14**, 2747-2754.
35. P. M. A. Caetano, A. S. Albuquerque, L. E. Fernandez-Outon, W. A. A. Macedo and J. D. Ardisson, *J. Alloys Compd.*, 2018, **758**, 247-255.
36. C. Schliehe, J. Yuan, S. Glatzel, K. Siemensmeyer, K. Kiefer and C. Giordano, *Chem. Mater.*, 2012, **24**, 2716-2721.
37. M. Mikhaylova, D. K. Kim, N. Bobrysheva, M. Osmolowsky, V. Semenov, T. Tsakalakos and M. Muhammed, *Langmuir*, 2004, **20**, 2472-2477.
38. K. Soulantica, F. Wetz, J. Maynadie, A. Falqui, R. P. Tan, T. Blon, B. Chaudret and M. Respaud, *Appl. Phys. Lett.*, 2009, **95**, 152504/152501-152504/152503.
39. J. M. Asensio, J. Marbaix, N. Mille, L.-M. Lacroix, K. Soulantica, P.-F. Fazzini, J. Carrey and B. Chaudret, *Nanoscale*, 2019, DOI: 10.1039/C1038NR10235J
40. B. Cormary, T. Li, N. Liakakos, L. Peres, P.-F. Fazzini, T. Blon, M. Respaud, A. J. Kropf, B. Chaudret, J. T. Miller, E. A. Mader and K. Soulantica, *J. Am. Chem. Soc.*, 2016, **138**, 8422-8431.
41. C. Blanco-Andujar, D. Ortega, P. Southern, Q. A. Pankhurst and N. T. K. Thanh, *Nanoscale*, 2015, **7**, 1768-1775.
42. V. Connord, B. Mehdaoui, R. P. Tan, J. Carrey and M. Respaud, *Rev. Sci. Instrum.*, 2014, **85**, 093904/093901-093904/093908.
43. L.-M. Lacroix, S. Lachaize, A. Falqui, M. Respaud and B. Chaudret, *J. Am. Chem. Soc.*, 2009, **131**, 549-557.